SCIENTIFIC REPORTS

OPEN

SUBJECT AREAS:
COMPLEX NETWORKS
STATISTICAL PHYSICS
EVOLUTIONARY THEORY

Received
3 December 2014

Accepted
2 March 2015

Published
23 March 2015

Correspondence and requests for materials should be addressed to Y.K. (ykim@khu.ac.kr)

Spatial evolutionary public goods game on complete graph and dense complex networks

Jinho Kim, Huiseung Chae, Soon-Hyung Yook & Yup Kim

Department of Physics and Research Institute for Basic Sciences, Kyung Hee University, Seoul 130-701, Korea.

We study the spatial evolutionary public goods game (SEPGG) with voluntary or optional participation on a complete graph (CG) and on dense networks. Based on analyses of the SEPGG rate equation on finite CG, we find that SEPGG has two stable states depending on the value of multiplication factor r, illustrating how the "tragedy of the commons" and "an anomalous state without any active participants" occurs in real-life situations. When r is low ($r \ll r^*$), the state with only loners is stable, and the state with only defectors is stable when r is high ($r \gg r^*$). We also derive the exact scaling relation for r^*. All of the results are confirmed by numerical simulation. Furthermore, we find that a cooperator-dominant state emerges when the number of participants or the mean degree, $\langle k \rangle$, decreases. We also investigate the scaling dependence of the emergence of cooperation on r and $\langle k \rangle$. These results show how "tragedy of the commons" disappears when cooperation between egoistic individuals without any additional socioeconomic punishment increases.

The emergence and evolution of cooperation is central to understanding the evolution and human activity-associated dynamics. One of the most popular theoretical frameworks that is used to shed light on such issues is evolutionary game theory. Game theory has also been successfully applied in diverse fields such as evolutionary biology and psychology[1], computer science and operations research[2,3], political science and military strategy[4,5], cultural anthropology[6], ethics and moral philosophy[7], economics[8,9], traffic flow research[10,11] and public health[12]. When preferences and goals of participating agents are in conflict, game theory can explain and predict interactive decisions[13]. The central aim of game theory research is to determine conditions needed for cooperation to emerge between egoistic individuals[14–16]. Two of the most famous models for game theory include the prisoner's dilemma (PD) and public goods game (PGG)[17]. While the PD for a pairwise interaction attracted the attention of biologists and social scientists, PGG for group interactions was the focus of studies in experimental economics[18]. The PGG was often studied to identify effects of collective action arising from joint group decisions. Although sometimes the group interactions can be modeled as repeated simple pair interactions as with the PD, the most fundamental unit of the game is irreducible multi-agent nature[13,19,20]. The PGG offers valuable insight into prevailing socioeconomic problems such as pollution, deforestation, mining, fishing, climate control and environmental protection[13]. In identifying potential solutions to these issues, PGGs with various strategies[13,17,20–47] have been suggested and studied. Economists have mainly studied PGG with two strategies, C and D, in which all agents participate and share a single common pool[21–24].

In this report, we focus on a PGG with voluntary participation[25] in which three strategic players (cooperators (C), defectors (D) and loners (L)) are considered. Each C contributes c to the common pool, whereas D attempts to exploit the resource at no cost. Then, each C gets the payoff P_C as $P_C = rcn_C/(n_C + n_D) - c$, whereas each D obtains P_D as $P_D = rcn_C/(n_C + n_D)$. Here, n_C (n_D) denotes the number of C's (D's) participating in the game, and $r(>1)$ is the multiplication factor, which describes synergistic effects of cooperation. In contrast, L refuses to participate in the game and relies only on private payoff σ. In this report the condition, $0 < \sigma < c(r-1)$, is imposed[25].

Recently, the spatial evolutionary PGG (SEPGG) has been intensively studied to understand how steady-state strategies emerge on various structures and to identify characteristic features of such steady-state strategies[17,25,26,28–33]. In the SEPGG, each agent is assigned to a node on a lattice or network. In a unit game of the SEPGG, only a randomly selected agent and its linked neighbors participate[26]. Then, in each update of the SEPGG, a randomly selected agent i adopts the strategy of a randomly selected neighbor j of i with a transition probability f_{ij} that depends on payoffs P_i and P_j[17]. The SEPGG studies have revealed interesting results such as cyclic dominance[25,27], transition nature[26], and payoff distribution[28]. The effects of underlying topology on the

SEPGG properties[17,28–33] have also been found, such as the spatial reciprocity on diluted networks[34] and multiplex networks[35–40].

Since the SEPGG on regular lattices and sparse networks has considered only local interactions, the number of participants in a unit game centered at a node i cannot exceed $k_i + 1$, where k_i is the degree (or coordination number) of i. Thus, the SEPGG on sparse networks is hardly a theoretical model of real-life examples with very large participants such as taxes, provision levels, tolls, user fees, etc.[48]. Such cases involving public resources which anyone can overuse can be mapped into "tragedy of the commons" problem[49,50]. However, SEPGG in which all agents participate in a unit game has been rarely studied. Thus, we focus on SEPGG with very large participants.

In this report, the SEPGG with three strategies on a complete graph (CG) and dense complex networks is considered to understand the SEPGG with large participants. The CG is a simple undirected graph in which any node on the graph is linked to all other nodes. Thus, the number of links on the CG is $N(N-1)/2$, where N is the number of nodes. In the SEPGG on the CG, all agents participate in a unit game. From analytically exact rate equations of the SEPGG on the CG, two stationary states depending on r and N are found. The state with only L agents (or L-state) is stable for low $r(\ll r^*)$. The state with only D agents (or D-state) is stable for high $r(\gg r^*)$. r^* at which the crossover from the L-state to the D-state occurs is analytically obtained and also confirmed by numerical simulation. In the SEPGG on the CG, a C-dominant state cannot be stable even for very high r. These stationary states on the CG are very peculiar compared to the C-dominant state (or C-state) on regular lattices and sparse networks for very high r[28,30–33]. The L-state on the CG is also very peculiar in the sense that the L-state occurs only for $\sigma > c(r-1)$ in the PGG game with the well-mixed population[26], whereas the L-state on the CG occurs even when $0 < \sigma < c(r-1)$ or r is quite high.

More specifically, the time evolution of the SEPGG on the CG for high r is shown to have the following stages. In early time, the numbers of both C and L agents decrease, whereas the number of D agents hardly varies. Eventually, the D-state becomes stable. Hence, the time evolution of the SEPGG for high r describes key processes to the "tragedy of the commons" very well[49,50], because the key processes are the following processes: First, the most of agents overuse the public resource in the commons as defector. Then, the overuse of the public resource will ruin it.

Ref. 26 revealed that the dominant state on sparse networks for high r is the C-state. Hence, we investigate crossover behaviors of the L-state or the D-state on dense networks such as the CG to a C-state on sparse networks by numerical simulation. For low r, first the crossover from the L-state to a D-state occurs, and the D-state successively crosses over to a C-state as mean-degree $\langle k\rangle$ decreases. Furthermore, the D-state for moderate $\langle k\rangle$ remains even in the limit $N \to \infty$. We also quantitatively find that cooperation gradually increases as the number of participants or $\langle k\rangle$ decreases, which is the origin of two crossovers. Hence, the crossovers for low r describe how the enhanced cooperation on sparse networks with low $\langle k\rangle$ overcomes "tragedy of the commons", resulting in the C-state. For high r the direct crossover from the D-state to the C-state occurs. This direct crossover is nearly the same as that from the D-state to the C-state for low r.

Results

SEPGG on the complete graph. From f_{ij} in Eq. (11) using $\{P_i\}$ on the CG, exact rate equations of densities on the CG are written as

$$\dot{\rho}_C = \rho_C\rho_D \tanh\left[-\frac{\beta}{2}c\right] + \rho_C\rho_L \tanh\left[\frac{\beta}{2}\left(\frac{rc\rho_C}{1-\rho_L} - c - \sigma\right)\right], \quad (1)$$

$$\dot{\rho}_D = \rho_C\rho_D \tanh\left[\frac{\beta}{2}c\right] + \rho_D\rho_L \tanh\left[\frac{\beta}{2}\left(\frac{rc\rho_C}{1-\rho_L} - \sigma\right)\right], \quad (2)$$

and

$$\dot{\rho}_L = \rho_C\rho_L \tanh\left[\frac{\beta}{2}\left(c + \sigma - \frac{rc\rho_C}{1-\rho_L}\right)\right] + \rho_D\rho_L \tanh\left[\frac{\beta}{2}\left(\sigma - \frac{rc\rho_C}{1-\rho_L}\right)\right], \quad (3)$$

where $\dot{\rho}_C = d\rho_C/dt$, etc.

To obtain stationary states from general initial configurations with $\rho_C^I = \rho_C(t=0) > 0$, $\rho_D^I > 0$ and $\rho_L^I > 0$, early time behaviors of ρ_C, ρ_D, and ρ_L must be considered. Early time behaviors of ρ_C, ρ_D, and ρ_L are determined based on competition between two terms of Eqs. (1)–(3), respectively. As $\rho_C\rho_D \tanh(-\beta c/2) \le 0$ in Eq. (1) and $\rho_C\rho_D \tanh(\beta c/2) \ge 0$ in Eq. (2) for any non-negative ρ_C, ρ_D, β and c, two distinctive steady states are achievable depending on the value of ρ_C. When $\rho_C > (c+\sigma)\frac{1-\rho_L}{cr}\left(> \sigma\frac{1-\rho_L}{cr}\right)$, $\tanh\left[\frac{\beta}{2}\left(\frac{rc\rho_C}{1-\rho_L} - c - \sigma\right)\right] > 0$ in Eq. (1), $\tanh\left[\frac{\beta}{2}\left(\frac{rc\rho_C}{1-\rho_L} - \sigma\right)\right] > 0$ in Eq. (2), and $\tanh\left[-\frac{\beta}{2}\left(\frac{rc\rho_C}{1-\rho_L} - c - \sigma\right)\right] < 0$ in Eq. (3). Thus, $\dot{\rho}_D > 0$ and $\dot{\rho}_L < 0$, which make $\rho_C\rho_L \tanh\left[\frac{\beta}{2}\left(\frac{rc\rho_C}{1-\rho_L} - c - \sigma\right)\right] \ll 1$ in Eq. (1) and $\dot{\rho}_C < 0$ after some time. From these relations we find that the state of $\{\rho_D \simeq 1, \rho_C \ll 1, \rho_L \ll 1\}$ appears when $\rho_C > (c+\sigma)\frac{1-\rho_L}{cr}$. Similarly, when $(c+\sigma)\frac{1-\rho_L}{cr} > \rho_C > \sigma\frac{1-\rho_L}{cr}$, $\dot{\rho}_D > 0$ and $\dot{\rho}_C < 0$, which also make $\rho_C\rho_L \tanh\left[-\frac{\beta}{2}\left(\frac{rc\rho_C}{1-\rho_L} - c - \sigma\right)\right] \ll 1$ in Eq. (3) and $\dot{\rho}_L < 0$ after some time. As a result, when $\rho_C > \sigma\frac{1-\rho_L}{cr}$, the state of $\{\rho_D \simeq 1, \rho_C \ll 1, \rho_L \ll 1\}$ appears. We call this state the D-state. In contrast, when $\rho_C < \sigma\frac{1-\rho_L}{cr}$, $\dot{\rho}_L > 0$ and $\dot{\rho}_C < 0$, which make $\rho_C\rho_D \tanh\left(\frac{\beta c}{2}\right) \ll 1$ in Eq. (2) and $\dot{\rho}_D < 0$ after some time. Thus, the state of $\{\rho_L \simeq 1, \rho_C \ll 1, \rho_D \ll 1\}$ appears. We call this state the L-state. As the D-state or the L-state appears depending on the condition $\rho_C < \sigma\frac{1-\rho_L}{cr}$, we now examine the stability of the D-state based on rate equations (1)–(3). If the D-state is unstable, the L-state should be stable.

In the D-state with $\{\rho_D \simeq 1, \rho_C \ll 1, \rho_L \ll 1\}$, the rate equation (1) becomes

$$\dot{\rho}_C \simeq \rho_C \tanh\left(-\frac{\beta}{2}c\right), \quad (4)$$

because $\rho_L \ll \rho_D$. By solving Eq. (4) for time t, we obtain

$$\rho_C(t) \sim \exp\left[-\tanh\left(\frac{\beta}{2}c\right)t\right]. \quad (5)$$

Similarly, the rate equation (3) also becomes

$$\dot{\rho}_L \simeq -\rho_L \tanh\left[\frac{\beta}{2}\left(\frac{rc\rho_C}{1-\rho_L} - \sigma\right)\right]. \quad (6)$$

When $\rho_C \gg \sigma\frac{1-\rho_L}{cr}$, $\tanh\left[\frac{\beta}{2}\left(\frac{rc\rho_C}{1-\rho_L} - \sigma\right)\right] \simeq 1$ and

$$\rho_L(t) \sim \exp(-t). \quad (7)$$

As ρ_C decreases with t, the condition $\rho_C > \sigma\frac{1-\rho_L}{cr}$ for the D-state breaks down for $t > t^*$. From the Eq. (5) and the condition $\rho_C \sim \sigma\frac{1-\rho_L}{cr}$ with $\rho_L \ll 1$, $t^* \sim \left(\ln\frac{rc}{\sigma}\right) \Big/ \tanh\left(\frac{\beta c}{2}\right)$. Therefore, on

the CG with $N \to \infty$, the L-state is the only stationary state. However, on the CG with finite N, the nonzero-minimum of ρ_L is $1/N$ and thus $\rho_L = 0$ if $\rho_L(t) < 1/N$. Therefore, if $\rho_L(t^*) \sim \left(\frac{rc}{\sigma}\right)^{-1/\tanh(\beta c/2)} < 1/N$, then $\rho_L(t > t^*) = 0$ and the D-state is still the stationary state. These results mean that the SEPGG on the CG with finite N has the following stationary state. For $r \gg r^*$, the D-state becomes stable, where

$$\left(\frac{r^* c}{\sigma}\right)^{-1/\tanh\left(\frac{\beta c}{2}\right)} \sim \frac{1}{N}, \tag{8}$$

or

$$r^* \sim \frac{\sigma}{c} N^{\tanh\left(\frac{\beta c}{2}\right)}. \tag{9}$$

More specifically, this D-state for high r or $r \gg r^*$ has never been found on regular lattices and sparse networks. As emphasized in our introductory remarks, this state also describes "tragedy of the commons" very well. In contrast, for $r \ll r^*$, the L-state becomes stable. This L-state for $r \ll r^*$ has never been found on regular lattices and sparse networks either. The L-state is also anomalous and surprising, because no body remains as an active participant in the PGG for $r \ll r^*$. No C-dominant stationary state is found on the CG even for high r. Compared to the C-dominant stationary states on a square lattice[17,26] and on sparse networks[28,30–33] for high r, the stationary states on the CG are unique and anomalous.

In Fig. 1, $\rho_C(t)$, $\rho_D(t)$, and $\rho_L(t)$ from a single run of simulation on the CG with $N = 10^5$ are plotted. $\rho_C(t)$ and $\rho_L(t)$ decay exponentially in the early time regardless of the r value. For $r \gg \frac{c}{\sigma} N^{\tanh\left(\frac{\beta c}{2}\right)}$, the time dependences of $\rho_C(t)$ and $\rho_L(t)$ are sustained throughout, and the stationary D-state eventually appears as shown in Fig. 1(a) ($r = 2000$). In contrast, when $r \ll \frac{c}{\sigma} N^{\tanh\left(\frac{\beta c}{2}\right)}$, $\rho_L(t)$ increases after some time or for $t > t^*$ and the L-state eventually appears as shown in Fig. 1(b) ($r = 60$). Hence, simulation data presented in Fig. 1 exactly reproduce the analytical results of rate equations (1)–(3). More specifically, early time behaviors of $\rho_L \sim \exp(-t)$ and $\rho_C \sim \exp\left[-\tanh\left(\frac{\beta c}{2}\right) t\right]$ are confirmed by fittings to simulation data as shown in Figs. 1(a) and 1(b). Furthermore, the crossover time t^* for $r = 60$ is $t^* = 8.86$ in Fig. 1(b), which is nearly identical to t^* obtained from $t^* \sim \left(\ln \frac{rc}{\sigma}\right) \Big/ \tanh\left(\frac{\beta c}{2}\right)$.

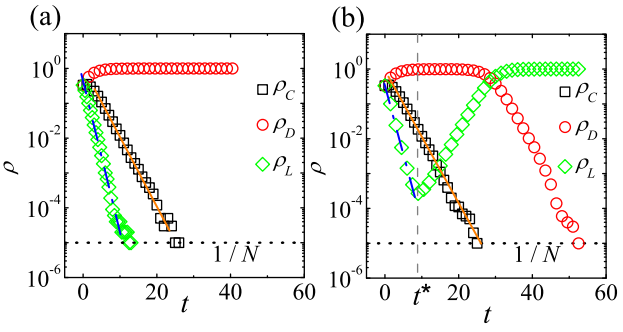

Figure 1 | Simulation results of the SEPGG on the CG. Plots of $\rho_C(t)$, $\rho_D(t)$, and $\rho_L(t)$ of the SEPGG with $c = 1$, $\sigma = 1$, and $\beta = 1$ from a single simulation run with $N = 10^5$. The dotted horizontal line denotes the value of $1/N$. (a) When $r = 2000$, the stationary D-state appears. By fitting the data to Eqs. (5) and (7), $\rho_C \sim \exp(\sim\alpha_C t)$ with $\alpha_C = 0.46(1)\left[\sim \tanh\left(\frac{\beta c}{2}\right)\right]$ (solid line) and $\rho_L \sim \exp(-\alpha_L t)$ with $\alpha_L = 1.00(2)(\sim 1.0)$ (dash-dotted line) are obtained. (b) When $r = 60$, the stationary L-state eventually appears. The vertical dashed line denotes the value of $t^*\left(\sim \left(\ln \frac{rc}{\sigma}\right) \Big/ \tanh\left(\frac{\beta c}{2}\right) \simeq 8.86\right)$. By the fitting, $\rho_C \sim \exp(-\alpha_C t)$ with $\alpha_C = 0.47(1)\left[\sim \tanh\left(\frac{\beta c}{2}\right) \simeq 0.4621\ldots\right]$ (solid line) and $\rho_L \sim \exp(-\alpha_L t)$ with $\alpha_L = 0.97(4)(\sim 1.0)$ (dash-dotted line) are obtained for $t < t^*$.

When $r \ll \frac{c}{\sigma} N^{\tanh\left(\frac{\beta c}{2}\right)}$ and in the limit of $N \to \infty$, the time dependences of ρ_C, ρ_D and ρ_L on the CG shown in Fig. 1(b) effectively present the process to the anomalous L-state with no active participants. The process means the following three steps. First, most agents defect one another. C then changes his strategy to D, and $\rho_C(t)$ decreases. Thus, D cannot receive enough payoff[50], causing $\rho_D(t)$ to decrease and $\rho_L(t)$ to increase. Finally, most agents become L, as no one remains in the commons. Consequently, the stationary L-state eventually appears for $r \ll \frac{c}{\sigma} N^{\tanh\left(\frac{\beta c}{2}\right)}$.

To analyze the dependence of stationary states on the multiplication factor r, $\rho_C^S = \rho_C(t \to \infty)$, $\rho_D^S = \rho_D(t \to \infty)$, and $\rho_L^S = \rho_L(t \to \infty)$ are obtained from simulations for various N and r by averaging over 1,000 realizations. Simulation results of ρ_D^S and ρ_L^S for various N and r are shown in the insets of Fig. 2. As shown in insets of Fig. 2, the crossover value of r, i.e., r^*, from the stationary L-state to the stationary D-state increases with N as expected from Eq. (9). More specifically, $\rho_D^S(N,r)$ and $\rho_L^S(N,r)$ in Fig. 2 exactly depend on the single scaling parameter r_0 defined as $r_0 \equiv rc \Big/ \left[\sigma N^{\tanh\left(\frac{\beta c}{2}\right)}\right]$. The scaling behaviors confirm that the L-state crosses over to the D-state at $r = r^* \sim \frac{\sigma}{c} N^{\tanh\left(\frac{\beta c}{2}\right)}$ as Eq. (9).

Crossover from the behavior on dense networks to that on sparse networks. A dense network is a network in which the mean-degree $\langle k \rangle$ satisfies $\langle k \rangle \propto N$[51]. For example, the CG is a typical dense network, as $\langle k \rangle = N - 1$ in the CG. In a sparse network, $\langle k \rangle = finite$[51]. In the SEPGG on the CG, either the L-state or the D-state is stable depending on r and N and the C-dominant state cannot be stable. In contrast, the C-dominant state is stable for relatively high r in the SEPGG on sparse networks such as random networks[30,33] and two dimensional square lattices[17,26]. Therefore, it is interesting to study how crossover from the L-state and the D-state on dense networks to the C-dominant state on sparse networks occurs for given values of r and N.

We first investigate how the L-state on dense networks crosses over to the C-dominant state on sparse networks. Since the L-state is stable for low r_0 on the CG as shown in Fig. 2, the crossover behaviors for low r_0 are studied by simulations on random networks with $\langle k \rangle$. For a given N and $\langle k \rangle$, ρ_C^S, ρ_D^S, and ρ_L^S are obtained by averaging over 2,000 realizations. Typical crossover behaviors for

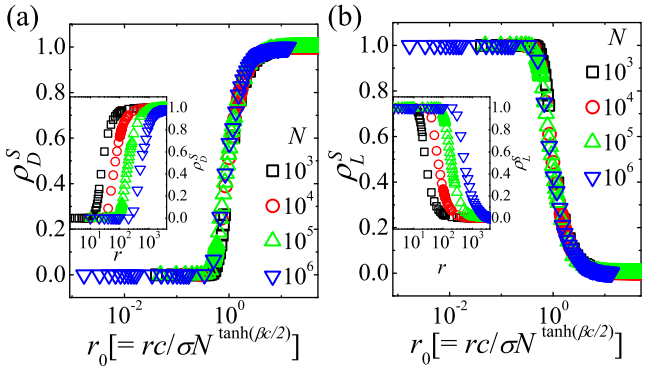

Figure 2 | Simulation results of the SEPGG on the CG for various r and N. Plots of (a) ρ_D^S and (b) ρ_L^S against $r_0\left(= rc \Big/ \left[\sigma N^{\tanh\left(\frac{\beta c}{2}\right)}\right]\right)$ for $N = 10^3$, 10^4, 10^5, and 10^6. $c = 1$, $\sigma = 1$, and $\beta = 1$ are used. Inset of (a): Plots of ρ_D^S against r. Inset of (b): Plots of ρ_L^S against r.

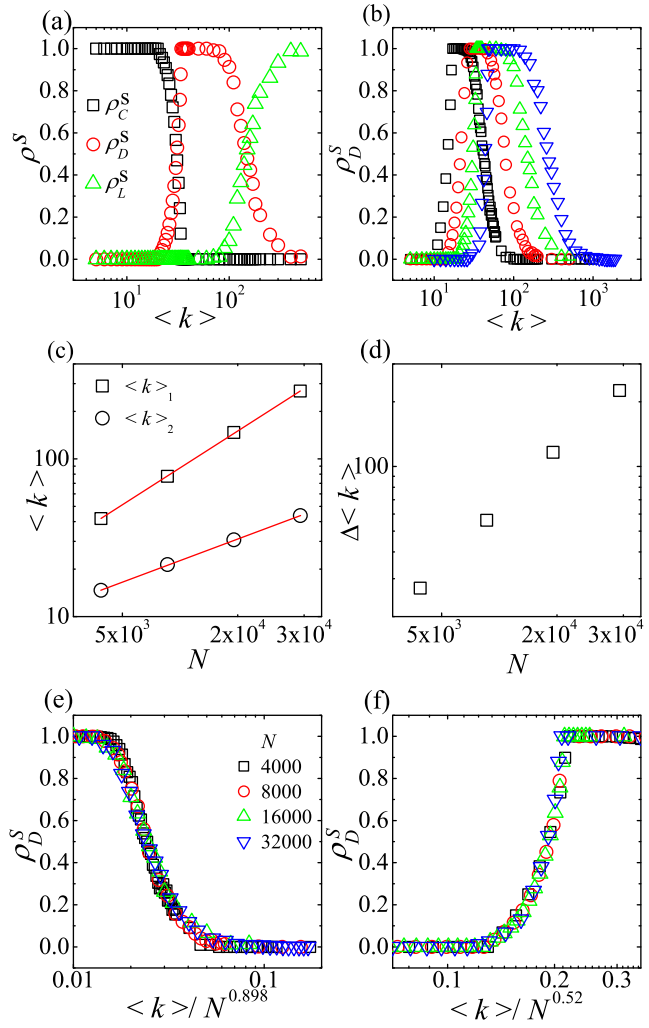

Figure 3 | Simulation results of the SEPGG on random networks for $r_0 = 0.3(\ll 1)$. (a) Plots of ρ_C^S, ρ_D^S, and ρ_L^S against $\langle k \rangle$ for $N = 16000$. $c = 1$, $\sigma = 1$, and $\beta = 1$ are used. (b) Plots of ρ_D^S against $\langle k \rangle$ for $N = 4000$, 8000, 16000, and 32000. Here, ρ_C^S and ρ_L^S are not shown, because $\rho_L^S = 1 - \rho_D^S$ for high $\langle k \rangle$ and $\rho_C^S = 1 - \rho_D^S$ for low $\langle k \rangle$. (c) Plots of $\langle k \rangle_1$ and $\langle k \rangle_2$ against N. The straight lines denotes fittings of $\langle k \rangle_1 = a_1 N^{\nu_1}$ with $\nu_1 \simeq 0.898(2)$ and $\langle k \rangle_2 = a_2 N^{\nu_1}$ with $\nu_2 \simeq 0.520(2)$ to corresponding data. (d) Plot of $\Delta \langle k \rangle$ ($\equiv \langle k \rangle_1 - \langle k \rangle_2$) against N. (e) Plot of ρ_D^S against $\langle k \rangle / N^{\nu_1}$ with ν_1 in (c). (f) Plot of ρ_D^S against $\langle k \rangle / N^{\nu_2}$ with ν_2 in (c).

$r_0 = 0.3$ are shown in Fig. 3. As shown in Fig. 3(a), two crossovers occur successively as $\langle k \rangle$ decreases. The L-state is stable when $\langle k \rangle$ is quite high. The C-state of $\{\rho_C^S = 1, \rho_D^S = 0, \rho_L^S = 0\}$ is stable when $\langle k \rangle$ is low enough. For moderate $\langle k \rangle$ the D-state is stable. Therefore, for low r_0, the stationary state is first changed from the L-state to a D-state and crossover from the D-state to a C-state occurs as $\langle k \rangle$ decreases.

The stability of the D-state for moderate $\langle k \rangle$ in the limit $N \to \infty$ is studied using the following methods. From simulation data of $\rho_C^s(\langle k \rangle, N)$, $\rho_D^s(\langle k \rangle, N)$ and $\rho_L^s(\langle k \rangle, N)$ as in Figs. 3(a) and 3(b), we first obtain $\langle k \rangle_1$ at which relations $\rho_L^S(\langle k \rangle_1, N) = 1/2$ and $\rho_D^S(\langle k \rangle_1, N) = 1/2$ hold simultaneously. We also obtain $\langle k \rangle_2$ at which $\rho_D^S(\langle k \rangle_2, N) = 1/2$ and $\rho_C^S(\langle k \rangle_2, N) = 1/2$ hold. For example, dependences of $\langle k \rangle_1$ and $\langle k \rangle_2$ on N for $r_0 = 0.3$ are shown in Fig. 3(c). The dependence of $\Delta \langle k \rangle$ ($\equiv \langle k \rangle_1 - \langle k \rangle_2$) is also shown in Fig. 3(d). As shown in Fig. 3(d), $\Delta \langle k \rangle$ increases monotonically with N, guaranteeing the stability of the D-state for moderate $\langle k \rangle$ in the limit $N \to \infty$. Furthermore, as shown in Fig. 3(c), $\langle k \rangle_1$ and $\langle k \rangle_2$ satisfy power laws $\langle k \rangle_1 \simeq N^{\nu_1}$ and $\langle k \rangle_2 \simeq N^{\nu_2}$. By fitting these power laws to data presented in Fig. 3(c), crossover exponents are obtained as $\nu_1 = 0.898(2)$, $\nu_2 = 0.520(2)$. The result $\nu_1 > \nu_2$ also guarantees the stability of the D-state for moderate $\langle k \rangle$. The crossover property from the L-state to the D-state presented in Fig. 3(b) is adequately described by the single exponent ν_1 obtained in Fig. 3(c). $\rho_D^S(\langle k \rangle, N)$'s for higher $\langle k \rangle$ and various N are plotted against the scaling variable $\langle k \rangle / N^{\nu_1}$ with the obtained ν_1 as in Fig. 3(e), which shows that $\rho_D^S(\langle k \rangle, N)$ for higher $\langle k \rangle$ is a function of the single scaling variable $\langle k \rangle / N^{\nu_1}$. As shown in Fig. 3(f), crossover from the D-state to the C-state also satisfies the scaling property that $\rho_D^S(\langle k \rangle, N)$ for lower $\langle k \rangle$ is a function of the single scaling variable $\langle k \rangle / N^{\nu_2}$ with the obtained exponent ν_2. Using the same method ν_1's and ν_2's for various low $r_0 (< 1)$ are obtained as shown in Fig. 4. Because $\nu_1 > \nu_2$ in Fig. 4, the D-state for moderate $\langle k \rangle$ and low $r_0 (< 1)$ is stable in the limit $N \to \infty$.

Furthermore, the dependences of ρ_C^S, ρ_D^S, and ρ_L^S on $\langle k \rangle$ for low r_0 in Fig. 3(a) are quite similar to the time dependences of $\rho_C(t)$, $\rho_D(t)$, and $\rho_L(t)$ on the CG for low r_0 shown in Fig. 1(b). In Fig. 1(b), initially there are enough Cs. As t increases, D governs the system. Finally L dominates, because D cannot receive enough payoff. Likewise, in Fig. 3(a), for low $\langle k \rangle$ there are also enough Cs. For moderate $\langle k \rangle$ D governs the system. When $\langle k \rangle$ becomes high enough, L dominates. Hence, it is very interesting to compare dynamical behaviors on the CG to static crossover behaviors depending on $\langle k \rangle$.

We thus now focus on the time dependence of $\rho_C(t)$, $\rho_D(t)$, and $\rho_L(t)$ for various $\langle k \rangle$ to understand crossover behaviors for low r_0 in Fig. 3(a). The time dependences of ρ_C, ρ_D, and ρ_L for moderate $\langle k \rangle$ are shown in Fig. 5(a), and those for low $\langle k \rangle$ are shown in Fig. 5(b). For high $\langle k \rangle$, the time dependence is nearly identical to that on the CG shown in Fig. 1(b). For moderate $\langle k \rangle$ and high $\langle k \rangle$, ρ_C and ρ_L decrease, but ρ_D increases in early time. However, the stationary state is strongly affected by the subsequent time dependence of ρ_C. If $\langle k \rangle$ is quite high or if $\langle k \rangle \gg \langle k \rangle_1$, ρ_C decays quickly and ρ_D cannot receive enough payoff. As a result, ρ_L increases for $t > t^*$ and the stationary L-state appears as explained in Fig. 1(b). In contrast, for moderate $\langle k \rangle$ or $\langle k \rangle_2 \ll \langle k \rangle \ll \langle k \rangle_1$, $\rho_C(t)$ decreases relatively slowly, and $\rho_L(t)$ never have a chance to increase reversely before the time at which $\rho_L(t) \leq 1/N$ [see Fig. 5(a)]. This means that the cooperation is effectively enhanced for moderate $\langle k \rangle$ and D receives enough payoff until L disappears due to the enhanced cooperation. This first crossover is quite similar to the crossover from the L-state in Fig. 1(b) to D-state in Fig. 1(a) on the CG. For low $\langle k \rangle$ or $\langle k \rangle \ll \langle k \rangle_2$, $\rho_C(t)$ never decreases as on sparse networks[28,30–33] [see Figs. 5(b)], and $\rho_C^S > \rho_D^S$. Hence, the crossover from the D-state to the C-state (or C-dominant state) occurs for $\langle k \rangle \sim \langle k \rangle_2$ as $\langle k \rangle$ decreases.

The two crossovers for low r_0 thus derive from a gradual increase of cooperation as the number of participants (or $\langle k \rangle$) decreases. Therefore, the crossovers that describe the disappearance of both the anomalous state with no active participants and "tragedy of the

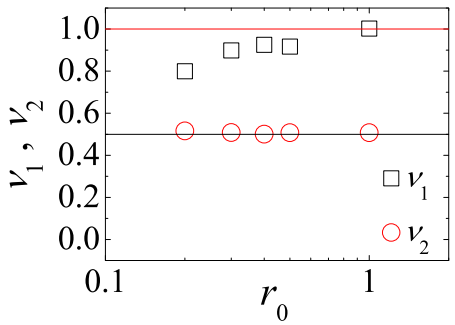

Figure 4 | Plots of exponents ν_1 and ν_2 against r_0. $c = 1$, $\sigma = 1$, and $\beta = 1$ are used. In the limit $N \to \infty$, the D-state for moderate $\langle k \rangle$ is stable, because $\nu_1 > \nu_2$.

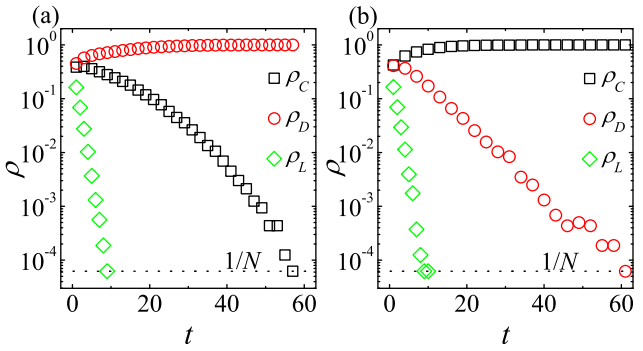

Figure 5 | Time dependence of $\rho_C(t)$, $\rho_D(t)$, and $\rho_L(t)$ on random networks with $N = 16000$ for $r_0 = 0.3$. Plots of $\rho_C(t)$, $\rho_D(t)$, and $\rho_L(t)$ (a) for moderate $\langle k\rangle$ (=30) and (b) for low $\langle k\rangle$ (=10). (a) For moderate $\langle k\rangle$ (=30), ρ_D increases with t, whereas ρ_C and ρ_L decreases. Finally, the stationary D-state emerges. (b) For low $\langle k\rangle$ (=10), ρ_C increases with t, whereas ρ_D and ρ_L decreases. Finally, the stationary C-state appears. The time dependences for high $\langle k\rangle$ are not shown, because they are nearly the same as those shown in Fig. 1(b).

commons" quantitatively show that agents in the larger group hardly cooperate relative to those in the smaller group[45,46]. However, this dependence on the group size is not necessarily accurate, because a recent study on PGG[44] reported that increasing the group size does not necessarily lead to mean-field behaviors.

Finally, we study the crossover from the D-state to a C-state for high $r_0(>1)$. Typical crossover behaviors for high r_0 are shown in Fig. 6(a). As shown in Fig. 6(a), for high $r_0(=10)$, the D-state is stable when $\langle k\rangle$ is quite high. The C-state is stable when $\langle k\rangle$ is low enough. Therefore, for high r_0, the direct crossover from the D-state to the C-state occurs as $\langle k\rangle$ decreases. To analyze the dependence of this direct crossover on N, $\rho_D^S(\langle k\rangle,N)'$s for various N are obtained by simulation as shown in Fig. 6(b). The dependence of the direct crossover on N can be obtained by the ansatz $\langle k\rangle_3 \sim N^{\nu_3}$, where at $\langle k\rangle_3$ both $\rho_D^S(\langle k\rangle_3,N) = 1/2$ and $\rho_C^S(\langle k\rangle_3,N) = 1/2$ hold. From the dependence of $\langle k\rangle_3$ on N, $\nu_3 \simeq 0.51(1)$ is obtained for $r_0 = 10$. This direct crossover satisfies the scaling property that $\rho_D^S(\langle k\rangle)$ is a function of the single scaling variable $\langle k\rangle/N^{\nu_3}$ with $\nu_3 = 0.51$. As shown in Fig. 6(d), ν_3's for various high $r_0(>1)$ are obtained using the same method. The data in Fig. 6(d) show that the value of ν_3 increases as r_0 increases. As the D-state is always stable on the CG or dense networks with $\langle k\rangle \propto N$, the upper bound of ν_3 should be equal to 1. We also confirm that the time dependences of $\rho_C(t)$, $\rho_D(t)$, and $\rho_L(t)$ for high r_0 are nearly the same as those in Fig. 1(a) for high $\langle k\rangle$ and as those in Fig. 5(b) for low $\langle k\rangle$, respectively. Hence, this direct crossover is nearly identical to the second crossover from the D-state to the C-state for low r_0.

Discussion

In summary, we have studied the SEPGG on the CG and complex dense networks to understand behaviors of the SEPGG with very large participants. By analyses of the rate equations, we have shown that the L-state of $\{\rho_C \ll 1, \rho_D \ll 1, \rho_L \simeq 1\}$ is stable on the CG for $r < r^*$ with $r^* \sim \frac{\sigma}{c} N^{\tanh\left(\frac{\beta c}{2}\right)}$. In contrast, the D-state of $\{\rho_C \ll 1, \rho_D \simeq 1, \rho_L \ll 1\}$, representing "tragedy of the commons", is stable for $r > r^*$. These analytic results on the CG have been confirmed by simulation.

We have also studied crossover behaviors from the L-state or the D-state on dense networks to the C-dominate state on sparse networks by numerical simulation on random networks with a mean degree $\langle k\rangle$. For $r < r^*$, the L-state first crosses over to a D-state, and successively this D-state crosses over to a C-state as $\langle k\rangle$ decreases. We have investigated the dependence of the crossovers on N for low r_0 using the ansatz $\langle k\rangle_1 \sim N^{\nu_1}$ and $\langle k\rangle_2 \sim N^{\nu_2}$, where the L-state is stable for $\langle k\rangle \gg \langle k\rangle_1$, the D-state is stable for $\langle k\rangle_2 \ll \langle k\rangle \ll \langle k\rangle_1$, and the

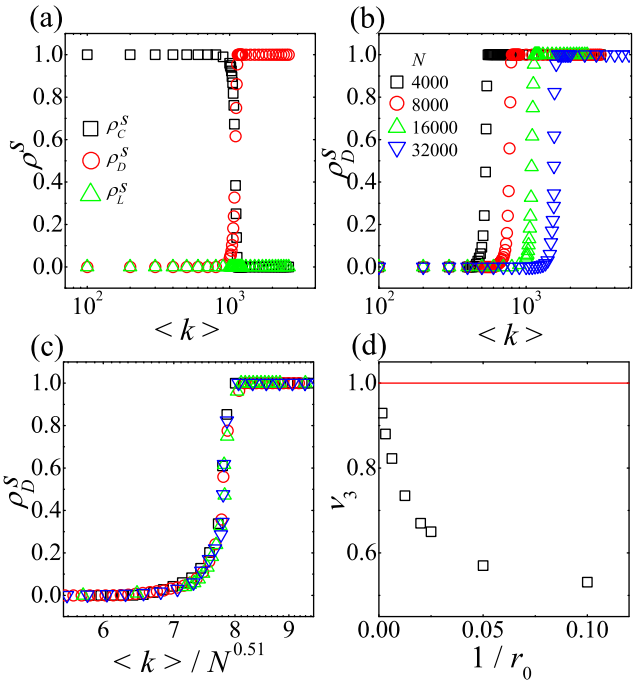

Figure 6 | Simulation results of the SEPGG on random networks for $r_0 = 10(\gg 1)$. (a) Plots of ρ_C^S, ρ_D^S, and ρ_L^S against $\langle k\rangle$ for $N = 16000$. $c = 1$, $\sigma = 1$, and $\beta = 1$ are used. The stationary state is changed from the D-state to a C-state as $\langle k\rangle$ decreases. $\rho_L^S = 0$ for any $\langle k\rangle$. (b) Plots of ρ_D^S against $\langle k\rangle$ for $N = 4000$, 8000, 16000, and 32000. (c) Plot of ρ_D^S against $\langle k\rangle/N^{\nu_3}$ with $\nu_3 \simeq 0.51$. (d) Plot of ν_3 against $1/r_0$.

C-state is stable for $\langle k\rangle \gg \langle k\rangle_2$. From the numerical simulations, ν_1 and ν_2 have been obtained. Since $\nu_1 > \nu_2$ for $r < r^*$, we have found that the D-state for moderate $\langle k\rangle$ is stable even in the limit $N \to \infty$. We have also studied the time dependences of ρ_C, ρ_D, and ρ_L on random networks with $\langle k\rangle$ to understand the crossover behaviors for $r < r^*$. For moderate $\langle k\rangle$, the D-state is stable, because ρ_C decreases relatively slowly. For low $\langle k\rangle$, cooperation is enhanced and the C-state is stable. The two crossovers for $r < r^*$ derive from a gradual increase of cooperation as the number of participants (or $\langle k\rangle$) decreases. The crossovers thus show how the enhanced cooperation on sparse networks with low $\langle k\rangle$ produces the C-state, overcoming both the anomalous state with no active participants and "tragedy of the commons" for low r_0.

For high r_0, the D-state is stable when $\langle k\rangle$ is high. The C-state is stable when $\langle k\rangle$ is low. Therefore, for high r_0, the direct crossover from the D-state to the C-state occurs as $\langle k\rangle$ decreases. The dependence of the direct crossover on N has been also analyzed by the ansatz $\langle k\rangle_3 \sim N^{\nu_3}$, where the D-state appears for $\langle k\rangle \gg \langle k\rangle_3$ and the C-state appears for $\langle k\rangle \ll \langle k\rangle_3$. From the numerical simulations, ν_3 has been obtained. The value of ν_3 increases to 1 as r_0 increases, because the D-state always appears on the CG or dense networks with $\langle k\rangle \propto N$. The crossovers thus describe how the enhanced cooperation on sparse networks with low $\langle k\rangle$ overcomes "tragedy of the commons" and makes the C-state for high r_0.

Finally, the cyclic dominance in Ref. 25 can also be found for very low r and $\langle k\rangle$. For example, for $r_0 = 0.1$, the crossover from the C-state to the cyclic dominance occurs at $\langle k\rangle \simeq 10$ on the network with the size $N = 10^4$. This crossover behavior is not explained quantitatively here, because the crossover occurs only on sparse networks.

Methods

Let us define the SEPGG model on a given graph or network in detail. Each agent is assigned to a node on the network. Variable s_i of the agent on node i represents the

strategy of i. The s_i is a cooperator (C), defector (D) or loner (L). The number of agents with a given strategy is denoted as $N_C\left(=\sum_{i=1}^{N}\delta_{s_i,C}\right)$, $N_D\left(=\sum_{i=1}^{N}\delta_{s_i,D}\right)$, and $N_L\left(=\sum_{i=1}^{N}\delta_{s_i,L}\right)$, where N is the size of the network.

In each update of SEPGG on the network, an agent i is randomly selected. Then, the payoff P_i of i depends on the strategies of k_i+1 participants, where k_i is the degree of i. If $n_{i,C}$ is the number of agents with C, $n_{i,D}$ is the number of agents with D, and $n_{i,L}$ is the number of agents with L among the k_i+1 participants, $n_{i,C}+n_{i,D}+n_{i,L}=k_i+1$. P_i is thus given by

$$P_i=\begin{cases}\frac{rcn_{i,C}}{n_{i,C}+n_{i,D}}-c & \text{if } s_i=C\\ \frac{rcn_{i,C}}{n_{i,C}+n_{i,D}} & \text{if } s_i=D\\ \sigma & \text{if } s_i=L\end{cases}. \tag{10}$$

Here, c is the cost contributed by a C to the common pool, $r(>1)$ is the multiplication factor and σ is the fixed payoff of a L[26]. We impose the condition $0<\sigma<c(r-1)$ as in Ref. 25. Even if only one active participant remains, the payoff of the agent still follows Eq. (10). Then, the strategy of i is updated through the comparison of P_i with P_j of a randomly selected neighbor j among k_i neighbors in order to select a better strategy. If $s_i\neq s_j$, the agent i stochastically adopts the strategy s_j of the neighbor j with transition probability f_{ij}. We use

$$f_{ij}=\frac{\exp(\beta P_j)}{\exp(\beta P_j)+\exp(\beta P_i)}, \tag{11}$$

as in Ref. 17. Here $\beta(\geq 0)$ controls the amount of noise. In each update of SEPGG, the payoffs in f_{ij} of Eq. (11) on regular lattices and sparse networks depend on the configuration of all the agents at the time of the update. In contrast, P_i in f_{ij} on the CG depends only on s_i and N_C, N_D, and N_L, of the strategies on the entire graph, because all agents participate in each unit game. The payoff $\{P_i\}$ on the CG is thus written as

$$\begin{aligned}P_i(s_i=C)&=P_C=\tfrac{rc\rho_C}{\rho_C+\rho_D}-c\\ P_i(s_i=D)&=P_D=\tfrac{rc\rho_C}{\rho_C+\rho_D}\\ P_i(s_i=L)&=P_L=\sigma\end{aligned}, \tag{12}$$

where the densities $\rho_C(\equiv N_C/N)$, $\rho_D(\equiv N_D/N)$, and $\rho_L(\equiv N_L/N)$ are used. To confirm the analytic results, simulations are performed for various N and r. Here, we mainly report the results of simulations with $\rho_C^I=\rho_D^I=\rho_L^I=1/3$, $c=1$, $\sigma=1$ and $\beta=1$. Simulations with various combinations of ρ_C^I, ρ_D^I, ρ_L^I, c, σ and β are tested and nearly identical results are obtained.

1. Smith, J. M. & Price, G. R. The logic of animal conflict. *Nature* **246**, 15–18 (1973).
2. Ben-David, S., Borodin, A., Karp, R., Tardos, G. & Wigerson, A. On the power of randomization in on-line algorithms. *Algorithmica* **11**, 2–14 (1994).
3. Frederic, S. H. & Gerald, J. L. *Introduction to operations research* (Mc Graw Hill, 2010).
4. Downs, A. *An economic theory of democracy* (Harper and Row, New York, 1957).
5. Melvin, D. *Games of strategy: Theory and applications* (RAND corporation, 2007).
6. Henrich, J. *et al. Foundations of human sociality: Economic experiments and ethnographic evidence from fifteen small-scale societies* (Oxford University Press, New York, 2004).
7. Quine, W. V. Carnap and logical truth. *Synthese* **12**, 350–374 (1960).
8. Neumann, J. & Morgenstern, O. *Theory of games and economic behavior* (Princeton university press, Princeton, 1953).
9. Friedman, J. W. *Game theory with applications to economics* (Oxford university press, New York, 1990).
10. Tanimoto, J., Fujiki, T., Wang, Z., Hagishima, A. & Ikegaya, N. Dangerous drivers foster social dilemma structures hidden behind a traffic flow with lane changes. *J. Stat. Mech.* **1742–5468**, P11027 (2014).
11. Perc, M. Premature seizure of traffic flow due to the introduction of evolutionary games. *New. J. Phys.* **9**, 3 (2007).
12. Wang, Z., Zhang, H. & Wang, Z. Multiple effects of self-protection on the spreading of epidemics. *Chaos, Solitons & Fractals* **61**, 1 (2014).
13. Szabó, G. & Fáth, G. Evolutionary games on graphs. *Phys. Rep.* **446**, 97–216 (2007).
14. Axelrod, R. *The evolution of cooperation* (Basic Books, New York, 1984).
15. Maynard, S. J. *Evolution and the theory of game* (Cambridge university press, Cambridge, England, 1982).
16. Nowak, M. *Evolutionary dynamics: Exploring the equation of life* (Harvard university, Cambridge, MA, 2006).
17. Hauert, C. & Szabo, G. Game theory and physics. *Am. J. Phys.* **73**, 405 (2005).
18. Kagel, J. H. & Roth, A. E. *The Handbook of Experimental Economics* (Princeton University Press, Princeton, 1995).
19. Pacheco, J. M., Santos, F. C., Souza, M. O. & Skyrms, B. Evolutionary Dynamics of Collective Action in n-person stag hunt dilemmas. *Proc. R. Soc. B* **276**, 315–321 (2009).
20. Perc, M., Gomez-Gardenes, J., Szoloki, A., Floria, M. L. & Moreno, Y. Evolutionary dynamics of group interactions on structured populations: a review. *J. R. Soc. Interface* **10**, 20120997 (2013).
21. Ledyard, J. O. *Public goods: a survey of experimental research* (Princeton University Press, Princeton, 1995).
22. Fehr, E. & Gächter, S. Cooperation and Punishment in Public Goods Experiments. *Am. Econ. Rev.* **90**, 980–994 (2000).
23. Fischbacher, U., Gächter, S. & Fehr, E. Are people conditionally cooperate? Evidence from a public goods experiment. *Econ. Lett.* **71**, 397–404 (2001).
24. Fehr, E. & Gächter, S. Altruistic punishment in humans. *Nature* **415**, 137–140 (2002).
25. Hauert, C., De Monte, S., Hofbauer, J. & Sigmund, K. Volunteering as Red queen mechanism for cooperation in public goods games. *Science* **296**, 1129–1132 (2002).
26. Szabo, G. & Hauert, C. Phase transitions and volunteering in spatial public goods games. *Phys. Rev. Lett.* **89**, 11801 (2002).
27. Szolnoki, A. *et al.* Cyclic dominance in evolutionary games: A review. *J. R. Soc. Interface* **11**, 20140735 (2014).
28. Francsco, C. S., Marta, D. S. & Jorge, M. P. Social diversity promotes the emergence of cooperation in public goods games. *Nature* **454**, 213–216 (2008).
29. Szabo, G. & Hauert, C. Evolutionary prisoner's dilemma games with voluntary participation. *Phys. Rev. E* **66**, 062903 (2002).
30. Szolnoki, A., Perc, M. & Szabo, G. Topology-independent impact of noise on cooperation in spatial public goods games. *Phys. Rev. E* **80**, 056109 (2009).
31. Yang, H., Wang, W., Wu, Z., Lai, Y. & Wang, B. Diversity-optimized cooperation on complex networks. *Phys. Rev. E* **79**, 056107 (2009).
32. Zhang, H., Liu, R., Wang, Z., Yang, H. & Wang, B. Aspiration-induced reconnection in spatial public-goods game. *Europhys. Lett.* **94**, 18006 (2011).
33. Ohtsuki, H., Hauertm, C., Lieberman, E. & Nowak, M. A A simple rule for the evolution of cooperation on graphs and social networks. *Nature* **441**, 502–505 (2006).
34. Wang, Z., Szolnoki, A. & Perc, M. Percolation threshold determines the optimal population density for public cooperation. *Phys. Rev. E* **85**, 037101 (2012).
35. Wang, Z., Szolnoki, A. & Perc, M. Rewarding evolutionary fitness with links between populations promotes cooperation. *J. Theo. Biol.* **349**, 50–56 (2014).
36. Wang, Z., Szolnoki, A. & Perc, M. Optimal interdependence between networks for the evolution of cooperation. *Sci. Rep.* **3**, 2470 (2013).
37. Boccaletti, S. *et al.* The structure and dynamics of multilayer networks. *Phys. Rep.* **544**, 1 (2014).
38. Wang, Z., Szolnoki, A. & Perc, M. Interdependent network reciprocity in evolutionary games. *Sci. Rep.* **3**, 1180 (2013).
39. Wang, Z., Szolnoki, A. & Perc, M. Evolution of public cooperation on interdependent networks: The impact of biased utility functions. *Europhys. Lett.* **97**, 48001 (2012).
40. Szolnoki, A., Wang, Z. & Perc, M. Wisdom of groups promotes cooperation in evolutionary social dilemmas. *Sci. Rep.* **2**, 576 (2013).
41. Helbing, D., Szolnoki, A. & Szabó, G. Evolutionary Establishment of Moral and Double Moral Standards through Spatial Interactions. *PLoS Comput. Biol.* **6**, e1000758 (2010).
42. Szolnoki, A., Szabó, G. & Cazkó, L. Competition of individual and institutional punishments in spatial public goods game. *Phys. Rev. E* **84**, 046106 (2011).
43. Szolnoki, A. & Perc, M. Correlation of positive and negative reciprocity fails to confer an evolutionary advantage: Phase transition to elementary strategies. *Phys. Rev. X* **3**, 041021 (2013).
44. Szolnoki, A. & Perc, M. Group-size effects on the evolution of cooperation in the spatial public goods game. *Phys. Rev. E.* **84**, 047102 (2011).
45. Isaac, R. M. & Walker, J. M. Group Size Effects in Public Goods Provision: The Voluntary contributions Mechanism. *Quart. J. Econ.* **103** 179–199 (1988).
46. Huang, Z.-G., Wu, Z.-X., Wu, A.-C., Yang, L. & Wang, Y.-H. Role of collective influence in promoting cooperation. *Euro. Phys. Lett.* **84**, 50008 (2008).
47. Chen, X., Szolnoki, A. & Perc, M. Probabilistic sharing solve the problem of costly punishment. *New. J. Phys.* **16**, 083016 (2014).
48. Cornes, R. & Sandler, T. *the theory of externalities public goods, and club goods* (Cambridge university press, Cambridge, England, 1986).
49. Hardin, G. The tragedy of the commons. *Science* **162**, 1243–1248 (1968).
50. Hardin, G. Extensions of "The Tragedy of the Commons" *Science* **280**, 682–683 (1998).
51. Newman, M. E. J. *Networks.* (Oxford university press, New York, 2010).

Acknowledgments

This research was supported by Basic Science Research Program through the National Research Foundation of Korea(NRF) funded by the Ministry of Science, ICT & Future Planning (NRF-2013R1A1A2057791 and NRF-2012R1A1A2007430).

Author contributions

J.K., H.C., S.-H.Y. and Y.K. designed the study; H.C. performed the analytic calculation; J.K. performed the simulations and analyzed data; H.C., S.-H.Y. and Y.K. wrote the manuscript. All authors revised the manuscript.

Additional information

Competing financial interests: The authors declare no competing financial interests.

How to cite this article: Kim, J., Chae, H., Yook, S.-H. & Kim, Y. Spatial evolutionary public

goods game on complete graph and dense complex networks. *Sci. Rep.* **5**, 9381; DOI:10.1038/srep09381 (2015).